

Constraints on axial two-body currents from solar neutrino data

A. B. Balantekin* and H. Yüksel†

Department of Physics, University of Wisconsin, Madison, Wisconsin 53706, USA

(Received 17 July 2003; published 12 November 2003)

We briefly review recent calculations of neutrino-deuteron cross sections within the effective field theory and traditional potential model approaches. We summarize recent efforts to determine the counter term describing axial two-body currents, L_{1A} , in the effective field theory approach. We determine the counterterm directly from the solar neutrino data and find several, slightly different, ranges of L_{1A} under different sets of assumptions. Our most conservative fit value with the largest uncertainty is $L_{1A}=4.5^{+18}_{-12}$ fm³. We show that the contribution of the uncertainty of L_{1A} to the analysis and interpretation of the solar neutrino data measured at the Sudbury Neutrino Observatory is significantly less than the uncertainty coming from the lack of having a better knowledge of θ_{13} .

DOI: 10.1103/PhysRevC.68.055801

PACS number(s): 13.15.+g, 23.40.Bw, 25.30.Pt, 26.65.+t

A significant amount of theoretical work was recently directed towards the calculation of neutrino capture on deuteron. Some of these efforts to describe this process utilized the effective field theory approach. In this approach nonlocal interactions at short distances are represented by effective local interactions in a derivative expansion. Since the effect of a given operator on low-energy physics is inversely proportional to its dimension, an effective theory valid at low energies can be written down by retaining operators up to a given dimension. The coefficients of these operators are then needed to be fixed either directly by the data or can be fitted to the results of calculations carried out using more traditional approaches.

For nucleon-nucleon interactions it was shown that one can introduce a well-defined power counting [1]. To describe the processes dominated by the isovector axial two-body current one needs to introduce a single coefficient, commonly called L_{1A} . This term then parametrizes the unknown axial current which plays a leading role in the description of the uncertainties of all neutrino-deuteron interactions. Using an effective theory without pions [2] such a calculation was carried out in Ref. [3]. These authors found that the ratio of charged- to neutral-current was fairly insensitive to this counterterm. To test the convergence of the results in Ref. [3] Butler, Chen, and Kong also calculated next-order corrections and found that no new parameters need to be introduced [4]. An alternative formulation of the effective field theory approach using heavy-baryon chiral perturbation theory was given in Ref. [5].

The cross section for neutrino absorption on deuterium was first calculated in Refs. [6,7] utilizing an effective range approximation to describe the nuclear interaction, using the allowed approximation for the weak operators, and assuming that the final two-nucleon state has a relative angular momentum of zero. First-forbidden contributions to the weak operators were included using Siegert's theorem in Ref. [8]

and using convection current form of the vector operators in Ref. [9]. A detailed assessment of various approximations in these papers was given in Refs. [10,11] using various nuclear potentials. This work was recently updated in Ref. [12].

Radiative corrections to the charged-current breakup of the deuteron were calculated by Towner in Ref. [13]. Beacom and Parke pointed out [14] inconsistencies in Towner's treatment of radiative corrections. This inconsistency was resolved in Ref. [15] and cross section calculations using more recent values of g_A were given in Refs. [15,16]. More recently it was shown that radiative corrections to the charged-current neutrino-nuclear reactions with either an electron or a positron in the final state are described by a universal function [17].

The counterterm L_{1A} describing the effects of the leading weak axial two-body current can be determined either by comparing various cross sections calculated using the effective field theory approach with those calculated using standard potential model approach or with experimentally or observationally determined cross sections. When the renormalization scale is set to the muon mass, dimensional analysis gives a rough estimate of this quantity [4],

$$|L_{1A}| \sim 6 \text{ fm}^3. \quad (1)$$

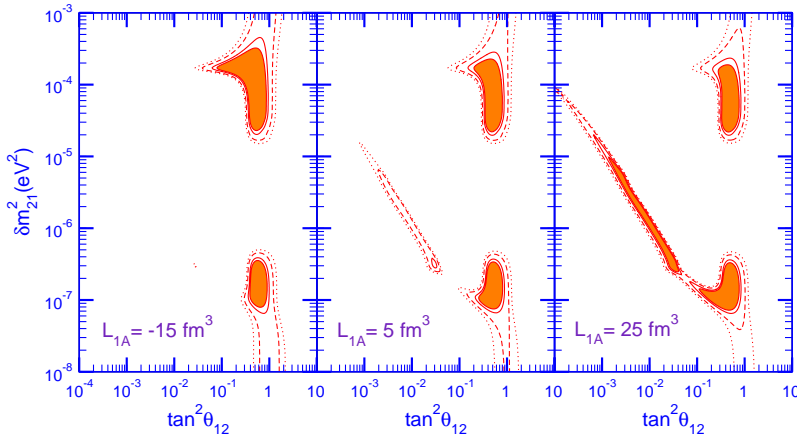
It should be emphasized that this number depends on the renormalization scale and cannot be reliably used at lower energies. Using the existing reactor antineutrino-deuteron breakup data provides a constraint of [18]

$$L_{1A} = 3.6 \pm 5.5 \text{ fm}^3. \quad (2)$$

Helioseismic observation of the pressure-mode oscillations of the Sun can be used to put constraints on various inputs into the standard solar model, in particular the pp fusion cross section. This process has been calculated to the fifth order in pionless effective field theory [19]. Neutrino-deuteron and antineutrino-deuteron scattering are computed to the third order in the same approach. The value of L_{1A} is not the same in different orders. Helioseismology limits $L_{1A}=7.0\pm 5.9$ fm³ in the fifth order [20]. Using the expressions given in Ref. [18] this gives

*Electronic address: baha@nucth.physics.wisc.edu

†Electronic address: yuksel@nucth.physics.wisc.edu



$$L_{1A} = 4.8 \pm 6.7 \text{ fm}^3 \quad (3)$$

in the third order. State of the art calculations of the pp fusion cross section are given in Refs. [21,22] where the uncertainty in the axial two-body current operator was adjusted to reproduce the measured Gamow-Teller matrix element of tritium β decay. After performing the transformation from the fifth to third order, the calculation of Ref. [21] indicates a value of

$$L_{1A} = 4.2 \pm 2.4 \text{ fm}^3. \quad (4)$$

One can also try to determine the counterterm directly using the solar neutrino data. Using the Sudbury Neutrino Observatory (SNO) and SuperKamiokande (SK) charged current, neutral current, and elastic scattering rate data, Chen, Heeger, and Robertson (CHR) find [23]

$$L_{1A} = 4.0 \pm 6.3 \text{ fm}^3. \quad (5)$$

In order to obtain this result CHR wrote the observed rate in terms of an averaged effective cross section and a suitably defined response function. In this paper we explore the phenomenology associated with the variation of L_{1A} .

In our calculations we used the neutrino cross sections given in Refs. [3] and [4]. The radiative corrections are taken into account following Ref. [15]. To calculate observed solar neutrino rates and spectra we used a covariance approach the details of which are described in Ref. [24]. In all calculations to obtain the Mikheyev-Smirnov-Wolfenstein (MSW) survival probabilities we used the neutrino spectra and solar electron density profile given by the standard solar model of Bahcall and collaborators [25].

The dependence of the extracted neutrino parameters on the value of L_{1A} is not very strong. We show how the parameter space changes with L_{1A} in Fig. 1. In this figure to find the allowed regions we fit 34 data points from the SNO day-night spectrum [26] using the procedure of Ref. [24]. The shaded area is the 90% confidence level region; 95% (solid line), 99% (long-dashed line), and 99.73% (dotted line) confidence levels are also shown. As L_{1A} changes from -15 fm^3 to 25 fm^3 we note that the changes in the shape of the confidence level intervals are small. In the calculations leading to this figure we took the total ${}^8\text{B}$ flux to be a free parameter using the procedure discussed in Ref. [24]. (Note

FIG. 1. (Color online) The change in the allowed region of the neutrino parameter space using solar neutrino data measured at SNO as the value of L_{1A} changes. In the calculations leading to this figure the neutrino mixing angle θ_{13} is taken to be zero (see text). The shaded areas are the 90% confidence level region; 95% (solid line), 99% (long-dashed line), and 99.73% (dotted line) confidence levels are also shown.

that even though we show the entire parameter space in this figure in the rest of this paper we concentrated on the large mixing angle region which is preferred by the global analysis). We conclude that the uncertainty in L_{1A} cannot be a significant source of error in the analysis of SNO data.

In general, both the deuteron breakup cross section and the total count rate at SNO are nonlinear in L_{1A} . Since L_{1A} is small the charged- and neutral-current count rates can be linearized by making a first-order expansion, i.e.,

$$\text{count rate} \sim A + B L_{1A}, \quad (6)$$

as was done by CHR. Both the energy dependence and the overall magnitude of the ${}^8\text{B}$ flux is an input into the standard solar model. The energy dependence is rather accurately determined by the laboratory measurements of the ${}^8\text{B}$ decay. The overall magnitude of this flux is determined by the rate of the ${}^7\text{Be}(p, \gamma){}^8\text{B}$ reaction in the Sun. This rate is extrapolated down from the measurements at laboratory energies (for a review, see Ref. [27]). To account for the sensitivity of the calculations on the value of the ${}^8\text{B}$ flux we set $\Phi({}^8\text{B}) = f_B \Phi_{\text{SSM}}({}^8\text{B})$ and calculate the total rate for various values of the parameter f_B . Clearly the total count rate should be proportional to the value of f_B . Note that the elastic scattering count rate is independent of L_{1A} . Thus allowing f_B to vary freely cannot be fully compensated by changing L_{1A} as we discuss below.

In Fig. 2 we present the quantity $\Delta\chi^2 = \chi^2 - \chi_{\text{min}}^2$ calculated as a function of L_{1A} . In this figure $\Delta\chi^2$ is projected only on one parameter (L_{1A}) so that $n\text{-}\sigma$ bounds on it are given by $\Delta\chi^2 = n^2$. θ_{13} is assumed to be zero. The solid line represents the case in which all other parameters (θ_{12} , δm_{12}^2 , and f_B) are unconstrained. The best fit value is given by $L_{1A} = 4.5 \text{ fm}^3$. In this case L_{1A} is constrained between -7 fm^3 and 23 fm^3 at 1σ level. Such a wide range is not surprising since the dependence of the rate on L_{1A} is small and the effects of the parameters such as θ_{12} , δm_{12}^2 , and f_B are much more dominant. In order to obtain a better bound on L_{1A} , we fix f_B so that the total count rate of SNO [26] is exactly reproduced at the value of L_{1A} which corresponds to the minimum χ^2 of the fit while the parameters θ_{12} and δm_{12}^2 are unconstrained. The resulting fit is shown by the dashed line. In this case L_{1A} is constrained between -2 fm^3 and 13 fm^3 at 1σ level. The dotted line in this figure represents the case where we fix all the

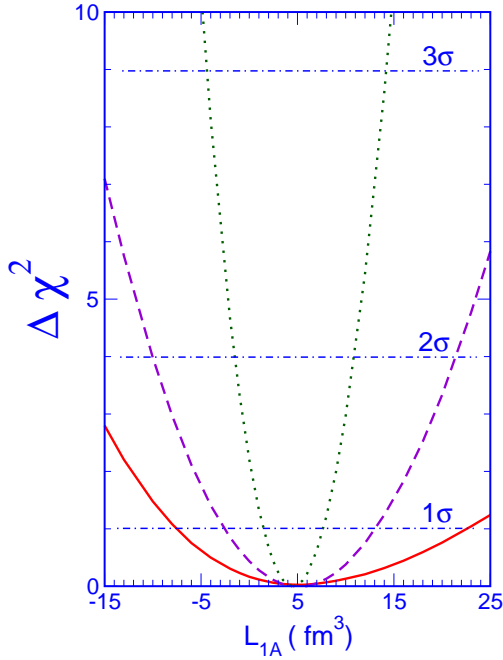


FIG. 2. (Color online) Projection of the global $\Delta\chi^2$ function on the parameter L_{1A} . In the calculations leading to this figure θ_{13} is taken to be zero. θ_{12} , δm_{12}^2 , and the parameter f_B (the multiplier of the ^8B flux) are varied. The solid line represents the case where all these three are unconstrained. The long-dashed line is when the ^8B flux is fixed as described in the text, but the other two are unconstrained. The dotted line is when θ_{12} and δm_{12}^2 are also taken to be the best fit values to the SNO energy spectra.

parameters except L_{1A} . We find the best fit values of θ_{12} and δm_{12}^2 in a global fit using 93 data points from solar and reactor neutrino experiments; namely, the total rate of the chlorine experiment (Homestake [28]), the average rate of the gallium experiments (SAGE [29], GALLEX [30], GNO [31]), 44 data points from the SK zenith-angle spectrum [32], 34 data points from the SNO day-night spectrum [26] and 13 data points from the KamLAND spectrum [33]. In addition we fix f_B so that the total count rate of SNO [26] is exactly reproduced. If we were to exclude SNO data from the global analysis and took $f_B=1$ instead of fixing as described above this method would be tantamount to treating SNO as an experiment to measure only L_{1A} so that the uncertainties in the SNO data would only show up as the corresponding uncertainty at L_{1A} . From the dotted line L_{1A} is constrained between 2 fm^3 and 8 fm^3 at 1σ level. In a sense this latter range represents the “best case” limit on L_{1A} that one can obtain from SNO. It is worth emphasizing that the χ^2 minimum is almost the same in all these cases. In all cases we obtain a best fit value of L_{1A} around $4.5\text{--}5 \text{ fm}^3$ which is a little larger than the value obtained by CHR. These authors use elastic scattering, charged-current, and neutral-current rates separately with effective cross sections. Since we fit the solar neutrino day-night spectrum directly by folding differential cross sections, detector response functions, ^8B spectrum, and the MSW survival probabilities, we need a slightly larger L_{1A} .

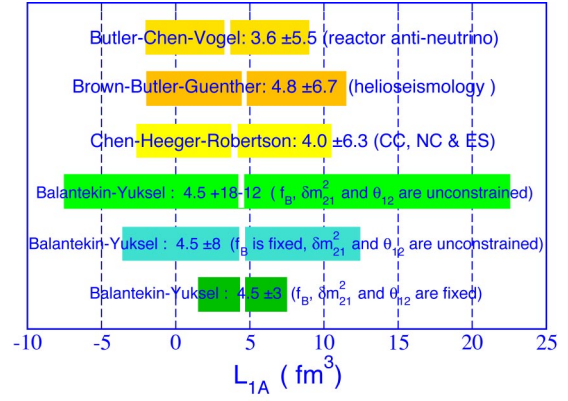


FIG. 3. (Color online) Values of L_{1A} obtained from different analyses. The values labeled Balantekin-Yuksel are calculated using the dashed and the dotted lines of Fig. 2 as described in the text. Helioseismology limit is from Ref. [20]. Reactor antineutrino limit is from Ref. [18]. The limit obtained by CHS [23] is also shown.

In Fig. 3 we compare our results with results from other analyses. Our results are based on the dashed and dotted lines of Fig. 2. We calculate 1σ errors by fitting a Gaussian of the form

$$\exp\left[-\frac{1}{2}\left(\frac{L_{1A} - L_{1A}^{\text{average}}}{\sigma_{L_{1A}}}\right)^2\right] \quad (7)$$

to each side of the marginal likelihood expression $\mathcal{L} = \exp(-\Delta\chi^2/2)$ and estimate two standard deviations separately for each side [34]. We obtain the error band shown in the figure by symmetrizing those errors.

One of the open questions in neutrino physics is understanding the role of mixing between the first- and third-flavor generations, θ_{13} . In this regard we also explored if the uncertainties coming from the lack of knowledge of θ_{13} and the counterterm L_{1A} are comparable. In the limiting case of small $\cos \theta_{13}$ and $\delta m_{31}^2 \gg \delta m_{21}^2$, which seems to be satisfied by the measured neutrino properties, it is possible to incorporate the effects of θ_{13} rather easily. In this limit the three-flavor survival probability is given by [35,36,24]

$$P_{3\times 3}(\nu_e \rightarrow \nu_e) = \cos^4 \theta_{13} P_{2\times 2}(\nu_e \rightarrow \nu_e \text{ with } N_e \cos^2 \theta_{13}) + \sin^4 \theta_{13}. \quad (8)$$

In Eq. (8) the quantity $P_{2\times 2}(\nu_e \rightarrow \nu_e \text{ with } N_e \cos^2 \theta_{13})$ is the standard two-flavor survival probability calculated with the modified electron density $N_e \cos^2 \theta_{13}$ and the standard initial conditions. This suggests that for small values of θ_{13} the survival probability and consequently the counting rate can be linearized in $\cos^4 \theta_{13}$:

$$\text{Count rate} \sim A + B(1 - \cos^4 \theta_{13}). \quad (9)$$

The neutral- and charged-current counting rates linearly depend on L_{1A} while elastic scattering rate does not. Conversely the charged-current and elastic scattering rates linearly depend on $\cos^4 \theta_{13}$ while the neutral-current rate does not. Hence it is reasonable to compare their relative

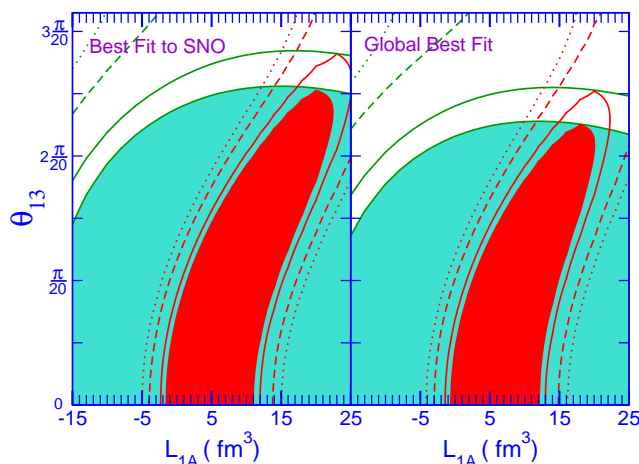


FIG. 4. (Color online) Allowed parameter space when θ_{12} and δm_{12}^2 are fixed to give the minimum χ^2 values to reproduce the SNO day-night spectrum (left-hand panel) and all solar neutrino experiments along with the KamLAND experiment (right-hand panel). The shaded areas are the 90% confidence level region; 95% (solid line), 99% (long-dashed line), and 99.73% (dotted line) confidence levels are also shown. The dark-shaded region corresponds to the case when the ^8B flux is fixed to be the standard solar model value. The light-shaded region corresponds to the case when that flux is unconstrained.

contributions. To this end in Fig. 4 we show the allowed θ_{13} and L_{1A} parameter space when θ_{12} and δm_{12}^2 are taken to give the minimum χ^2 values to reproduce the data. Results where the fixed values of θ_{12} and δm_{12}^2 obtained using only the best fit of the SNO data (left-hand panel) and using the best fit of all the solar neutrino data along with KamLAND results (right-hand panel) are both shown. The dark-shaded region corresponds to the case when $f_B=1$.

The light-shaded region corresponds to the case when the ^8B flux is unconstrained. We observe that the uncertainty coming from the lack of a better knowledge of θ_{13} is larger than uncertainty coming from not knowing L_{1A} precisely. One also observes that as θ_{13} increases the allowed L_{1A} region shifts toward larger values of L_{1A} . When $\theta_{13}=0$ the electron neutrino flux is lost into only one channel: a particular linear combination of μ and τ neutrinos [37]. But when $\theta_{13}\neq 0$ additional flux is lost into the orthogonal channel as well. The slightly decreased electron neutrino survival probability reduces the charged-current and the elastic scattering count rates so that a slightly larger L_{1A} is needed to compensate the resulting decrease in the count rates at each bin.

In conclusion we showed that the SNO experiment with increased statistics using additional input from other solar neutrino experiments can significantly reduce the uncertainty in determining the precise form of the axial two-body currents at low energies. We also showed that the contribution of the uncertainty in L_{1A} to the analysis and interpretation of the SNO data is nearly negligible. The effect of this uncertainty is smaller than the effects of a nonzero value of θ_{13} or even than the effects of possible solar density fluctuations [38]. Finally our most conservative value for L_{1A} is significantly larger than that was obtained by CHR. One reason for this may be the treatment of neutral- and charged-current count rates together in the global analysis.

We thank R.G.H. Robertson and Jiunn-Wei Chen for valuable comments on the first version of the paper and M. Butler for useful discussions and providing us the cross sections of Refs. [3] and [4]. This work was supported in part by the U.S. National Science Foundation Grant Nos. PHY-0070161 and PHY-0244384 and in part by the University of Wisconsin Research Committee with funds granted by the Wisconsin Alumni Research Foundation.

-
- [1] D. B. Kaplan, M. J. Savage and M. B. Wise, Phys. Lett. B **424**, 390 (1998).
 [2] D. B. Kaplan, M. J. Savage, and M. B. Wise, Phys. Rev. C **59**, 617 (1999); J. W. Chen, G. Rupak and M. J. Savage, Nucl. Phys. **A653**, 386 (1999); T. D. Cohen, Phys. Rev. C **55**, 67 (1997); P. F. Bedaque and U. van Kolck, Annu. Rev. Nucl. Part. Sci. **52**, 339 (2002).
 [3] M. Butler and J. W. Chen, Nucl. Phys. **A675**, 575 (2000).
 [4] M. Butler, J. W. Chen, and X. Kong, Phys. Rev. C **63**, 035501 (2001).
 [5] S. Ando, Y. H. Song, T. S. Park, H. W. Fearing, and K. Kubodera, Phys. Lett. B **555**, 49 (2003).
 [6] F. J. Kelly and H. Uberall, Phys. Rev. Lett. **16**, 145 (1966).
 [7] S. D. Ellis and J. N. Bahcall, Nucl. Phys. **A114**, 636 (1968).
 [8] S. Ying, W. Haxton, and E. M. Henley, Phys. Rev. D **40**, 3211 (1989).
 [9] N. Tataru, Y. Kohyama, and K. Kubodera, Phys. Rev. C **42**, 1694 (1990).
 [10] S. Ying, W. C. Haxton, and E. M. Henley, Phys. Rev. C **45**, 1982 (1992).
 [11] M. Doi and K. Kubodera, Phys. Rev. C **45**, 1988 (1992).
 [12] S. Nakamura, T. Sato, V. Gudkov, and K. Kubodera, Phys. Rev. C **63**, 034617 (2001).
 [13] I. S. Towner, Phys. Rev. C **58**, 1288 (1998).
 [14] J. F. Beacom and S. J. Parke, Phys. Rev. D **64**, 091302 (2001).
 [15] A. Kurylov, M. J. Ramsey-Musolf, and P. Vogel, Phys. Rev. C **65**, 055501 (2002).
 [16] S. Nakamura, T. Sato, S. Ando, T. S. Park, F. Myhrer, V. Gudkov, and K. Kubodera, Nucl. Phys. **A707**, 561 (2002).
 [17] A. Kurylov, M. J. Ramsey-Musolf, and P. Vogel, Phys. Rev. C **67**, 035502 (2003).
 [18] M. Butler, J. W. Chen, and P. Vogel, Phys. Lett. B **549**, 26 (2002).
 [19] M. Butler and J. W. Chen, Phys. Lett. B **520**, 87 (2001).
 [20] K. I. Brown, M. N. Butler, and D. B. Guenther, nucl-th/0207008.
 [21] R. Schiavilla *et al.*, Phys. Rev. C **58**, 1263 (1998).
 [22] T. S. Park *et al.*, Phys. Rev. C **67**, 055206 (2003); T. S. Park *et al.*, nucl-th/0106025.

- [23] J. W. Chen, K. M. Heeger and R. G. H. Robertson, *Phys. Rev. C* **67**, 025801 (2003).
- [24] A. B. Balantekin and H. Yuksel, *J. Phys. G* **29**, 665 (2003).
- [25] J. N. Bahcall, M. H. Pinsonneault, and S. Basu, *Astrophys. J.* **555**, 990 (2001).
- [26] Q. R. Ahmad *et al.*, SNO Collaboration, *Phys. Rev. Lett.* **87**, 071301 (2001); Q. R. Ahmad *et al.*, SNO Collaboration, *ibid.* **89**, 011302 (2002); Q. R. Ahmad *et al.*, *ibid.* **89**, 011301 (2002).
- [27] E. G. Adelberger *et al.*, *Rev. Mod. Phys.* **70**, 1265 (1998).
- [28] B. T. Cleveland *et al.*, *Astrophys. J.* **496**, 505 (1998).
- [29] J. N. Abdurashitov *et al.*, SAGE Collaboration, *Zh. Eksp. Teor. Fiz.* **122**, 211 (2002) [*JETP* **95**, 181 (2002)].
- [30] W. Hampel *et al.*, GALLEX Collaboration, *Phys. Lett. B* **447**, 127 (1999).
- [31] M. Altmann *et al.*, GNO Collaboration, *Phys. Lett. B* **490**, 16 (2000).
- [32] S. Fukuda *et al.*, Super-Kamiokande Collaboration, *Phys. Rev. Lett.* **86**, 5651 (2001); S. Fukuda *et al.*, Super-Kamiokande Collaboration, *ibid.* **86**, 5656 (2001).
- [33] K. Eguchi *et al.*, KamLAND Collaboration, *Phys. Rev. Lett.* **90**, 021802 (2003).
- [34] P. R. Bevington and D. K. Robinson, *Data Reduction and Error Analysis for the Physical Sciences* (McGraw-Hill, New York, 1992).
- [35] T. K. Kuo and J. Pantaleone, *Rev. Mod. Phys.* **61**, 937 (1989).
- [36] G. L. Fogli, E. Lisi, D. Montanino, and A. Palazzo, *Phys. Rev. D* **62**, 113004 (2000).
- [37] A. B. Balantekin and G. M. Fuller, *Phys. Lett. B* **471**, 195 (1999).
- [38] A. B. Balantekin and H. Yuksel, *Phys. Rev. D* **68**, 013006 (2003).